Thermal neutron scattering data for ^{7}LiF and BeF_2

Jia Wang[1,2], Hongzhou Song[1], Zehua Hu[1,2], Tao Ye[1], and Weili Sun[1,a]

[1] Institute of Applied Physics and Computational Mathematics, Beijing 100094, China
[2] Key Laboratory of Neutron Physics, CAEP, Mianyang 621900, China

Abstract. Based on the coherent elastic, incoherent elastic, coherent inelastic and incoherent inelastic scattering processes, a code named SIRIUS is developed to produce thermal neutron scattering data for crystals in ENDF-6 format. The phonon band structures and projected phonon densities of states of ^{7}LiF and BeF_2 crystals were calculated by Hellman-Feynman Theorem combined with a lattice dynamics direct method. Finally the thermal neutron scattering data for ^{7}LiF and BeF_2 crystals are given.

1. Introduction

Thermal neutron scattering data are widely used in nuclear engineering applications, such as reactor design, radiation shielding, long-lived nuclear waste transmutation, Boron Neutron Capture Therapy.

The study of thermal neutron scattering started from 1950s, which is due to the needs of the reactor design. Subsequently, GASKET code was developed at General Atomic [1,2], and was used to generate early thermal neutron scattering data. Now, LEAPR module in NJOY [3,4] code is widely used to calculate ENDF-6 format thermal neutron scattering law (TSL) data.

At present, some evaluated nuclear data libraries such as ENDF/B library [5], JENDL library [6], JEFF library [7] and IAEA nuclear data library contains the sublibrary of TSL data for about 23 moderators. However, new requirements for the development of current nuclear engineering, especially for the fourth generation reactor design need more TSL data. For example, in molten salt reactor, TSL data for Beryllium fluoride and Lithium fluoride are needed. Mei and Cai applied the CASTEP code and the modified NJOY code to generate the thermal neutron scattering data for LiF and BeF_2 crystals [8] and investigated the thermal neutron scattering data for molten salt Flibe based on the dynamic performance for Flibe [9]. To date, no thermal neutron scattering data in the ENDF format are available for Beryllium fluoride and Lithium fluoride.

Recently, a code named SIRIUS [10] is developed at IAPCM to generate the thermal neutron scattering data for solid in ENDF-6 format. In this paper, SIRIUS code is utilized to calculate the thermal neutron scattering data of ^{7}LiF and BeF_2 crystals.

2. Theoretical models

The theory of scattering of thermal neutron by crystals is exposed in details in many textbook [11,12] and is briefly considered here. There are four types of scattering, coherent elastic scattering, incoherent elastic scattering, coherent inelastic scattering and incoherent inelastic scattering.

The expression of the coherent elastic scattering cross section for polycrystalline material is

$$\sigma_{el,coh}(T) = \frac{\sigma_{coh}\pi^2\hbar^2}{2NV_0mE} \sum_{\tau} \frac{|F(N)|^2}{\tau} \exp(-4W(T)E_i) \quad (1)$$

The expression of the differential incoherent inelastic scattering cross section is

$$\frac{d\sigma_{el,inc}(T)}{d\Omega} = \frac{\sigma_{inc}}{4\pi} \exp(-2W(T)E(1-\mu)) \quad (2)$$

Where $W(T) = \frac{1}{Ak_BT}\int_0^{\beta_{max}} \frac{1}{\beta_s}\coth\left(\frac{\beta_s}{2}\right)\rho(\beta_s)d\beta_s$ is the Debye-Waller integral divided by the atomic mass, T is the temperature of the scattering medium, N and V_0 are the number of basis atoms and the volume of the primitive unit cell, respectively. m is the mass of the neutron, $|F(N)|$ is the crystallographic structure form factors, τ is the length of reciprocal vectors, E_i are the "Bragg edges", E is the incident neutron energies in the laboratory system, μ is the cosine of the scattering angle, the subscript coh means coherent and inc means incoherent. σ_{inc} and σ_{coh} are the incoherent and coherent bound scattering cross section for the material, respectively. For mixed moderator, the coherent elastic scattering cross section is more complicated and can be written as

$$\sigma_{el,coh}(T) = \frac{\pi^2\hbar^2}{2NV_0mE} \sum_{\tau} \frac{\left|\sum_{j-1}^{N}\sqrt{\sigma_{coh,j}}\exp(-2W_j(T)E_i)\exp(i2\pi\vec{\tau}_j\cdot\vec{d}_j)\right|^2}{\tau} \quad (3)$$

Where the subscript $j$means the jth atom in the unit cell. $\vec{\tau}$is the reciprocal lattice vector, $\vec{d}$ is atomic position of the

[a] e-mail: sun_weili@iapcm.ac.cn

jth atom. The calculation procedure for coherent elastic scattering of the mixed material goes as follows. Firstly, the $W_j(T)$ of all atoms are calculated separately. Secondly, the Eq. (3) is used to calculate the whole coherent elastic scattering cross section for the mixed moderator.

The expression of the double differential inelastic scattering cross section is

$$\left(\frac{d^2\sigma}{d\Omega dE'}\right)_{inl,inc} = \frac{1}{4\pi k_B T}\sqrt{\frac{E'}{E}}\exp(-\frac{\beta}{2}) \left(\sigma_{coh}S_{coh}(\alpha,\beta,T)+\sigma_{inc}S_{inc}(\alpha,\beta,T)\right) \tag{4}$$

k_B is the Boltzmann constant, $\alpha=E'+E-2\mu\sqrt{EE'}\Big/Ak_BT$ means the momentum transfer and $\beta = E' - E/k_BT$ means the energy transfer, $E'$is the scattering neutron energies in the laboratory system, $S(\alpha,\beta,T)$ is the thermal neutron scattering law.

$$\begin{aligned} S_{coh}(\alpha,\beta,T) &= S_d(\alpha,\beta,T) + S_s(\alpha,\beta,T) \\ S_{inc}(\alpha,\beta,T) &= S_s(\alpha,\beta,T) \end{aligned} \tag{5}$$

$S_s(\alpha,\beta,T)$ is know as the incoherent scattering law, and $S_d(\alpha,\beta,T)$ accounts for interference effects.

Generally, the interference effects in inelastic are considered so small that can be neglected, and the incoherent approximation is used [13]. The incoherent thermal neutron scattering law is given as

$$S_{inc}(\alpha,\beta,T) = \exp\left(-\beta/2\right)\exp(-\alpha\lambda)\sum_{p=1}^{\infty}\frac{1}{p!}\alpha^p F_p(\beta) \tag{6}$$

This expansion is known as the phonon expansion, subscript p represent the creation (or annihilation) of p phonons.where $\rho(\beta)$ is the phonon frequency distribution, $\lambda = \int_0^{\beta_{\max}} \frac{1}{\beta}\coth\left(\frac{\beta}{2}\right)\rho(\beta)d\beta$is the Debye-Waller integral,.

The $F_p(\beta)$ function is a convolution formula with

$$F_1(\beta) = \frac{\rho(\beta)}{\beta}\frac{\exp\left(\beta/2\right)}{2\sinh\left(\beta/2\right)}.$$

For strong coherent scatters such as graphite and beryllium, which means that the bound coherent scattering cross section is almost equal to the total bound scattering cross section, the incoherent approximation used in inelastic is known to introduce noticeable biases [14–17]. In these cases, the interference effects can't be neglected, so the thermal neutron scattering law is composed with coherent and incoherent contributions as follow

$$S(\alpha,\beta,T) = S_{coh,1p}(\alpha,\beta,T) + \sum_{i=2,p} S_{inc,i}(\alpha,\beta,T) \tag{7}$$

Here, only the one-phonon coherent is considered, the summation for the incoherent approximation starts from two phonons. The numerical formula of $S_{coh,1p}(\alpha,\beta,T)$ is given as

$$S_{coh,1p}(\alpha,\beta,\Delta\alpha,\Delta\beta,T) = \frac{3\hbar^2}{2Mk_BT}\exp\left(\frac{\beta}{2}\right)\frac{1}{\Delta\beta\beta} \frac{1}{\exp(\beta)-1}\sum_s \rho(\beta_s)\sum_{\vec{\kappa}}\frac{F_j^2\left(\vec{\kappa}\right)}{l(\alpha,\Delta\alpha)}\Delta\beta_s \tag{8}$$

where $F_j^2\left(\vec{\kappa}\right) = \left|\sum_d \exp(-W)\exp\left(i\vec{\kappa}\cdot\vec{d}\right)\left(\vec{\kappa}\cdot\vec{e_{ds}}\right)\right|^2$, $\vec{\kappa}$ is the scattering vector, $\vec{e_{ds}}$ is the polarisation vector of the$s$ model in position d, s stands for the double index $\vec{q}$ and j, j is the polarisation index (j = 1,2,3), $\vec{q}$ is the wavevector. The conditions $\vec{\kappa} = \vec{\tau} - \vec{q}$ and $\beta = \beta_s$ must be satisfied in the calculation. The calculated scattering law is an average value in $[\alpha, \alpha+\Delta\alpha]$ and $[\beta, \beta+\Delta\beta]$.

Finally, based on the theory, a code program SIRIUS is constructed to generate thermal neutrons scattering data in ENDF-6 format. In order to calculate coherent inelastic scattering, both the PDOSs and the phonon dispersion relation for materials are needed, otherwise, PDOSs for materials are enough.

3. Computational details

3.1. The phonon density of states

Beryllium fluoride (BeF_2) has a α-quartz-type structure and belongs to space group P3121 [18] with three beryllium atoms and six fluoride atoms in the unit cell.
Be: (0.4782, 0, 1/3), (0, 0.4782, 2/3), (0.5218, 0.5218, 0)
F: (0.4183, 0.2529, 0.2012), (0.7471, 0.1654, 0.5345)
(0.8346, 0.5817, 0.8678), (0.2529, 0.4183, 0.7988)
(0.1654, 0.7471, 0.4655), (0.5817, 0.8346, 0.1321)
The magnitude of reciprocal space vector of BeF_2 is

$$|\tau| = 2\pi\sqrt{4/3a^2\left(h^2+k^2+l^2\right)+1/c^2l^2} \tag{9}$$

Lithium fluoride (^{7}LiF) has a face centred cubic structure and belongs to space group FM3M [19] with four lithium atoms and four fluoride atoms in the unit cell.
F: (0, 0, 0), (0, 1/2, 1/2), (1/2, 0, 1/2), (1/2, 1/2, 0)
Li: (1/2, 1/2, 1/2), (1/2, 0, 0), (0, 1/2, 0), (0, 0, 1/2)
The magnitude of reciprocal space vector of ^{7}LiF is

$$|\tau| = \frac{2\pi\sqrt{\left(h^2+k^2+l^2\right)}}{a} \tag{10}$$

The computed lattice parameters of BeF_2 and ^{7}LiF are in well agreement with experimentally reported [20–22]. The lattice constants values for BeF2 are a = 4.85 Å, and c = 5.335 Å. The lattice constants value for ^{7}LiF is a = 4.026 Å. The structure for BeF_2 crystal and the structure for ^{7}LiF are showed in Fig. 1.

The phonon band structures and projected phonon densities of states of ^{7}LiF and BeF_2 crystals were calculated by Hellman-Feynman Theorem combined with a lattice dynamics direct method using the Vienna Ab inition Simulation Package (VASP) and the PHONON code [23,24]. For ^{7}LiF crystal, the model used a $3\times3\times3$ supercell composed of 216 atoms and for BeF_2

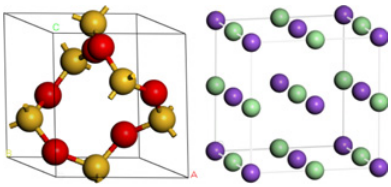

Figure 1. Structure of BeF_2 crystal (left)/^{7}LiF crystal (right).

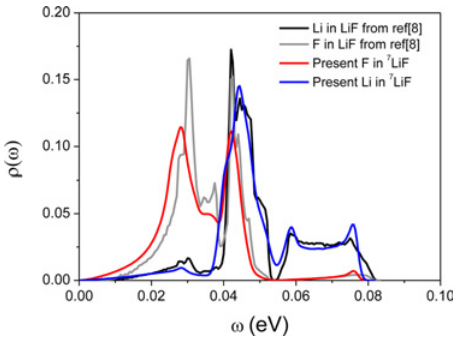

Figure 2. The calculated partial PDOSs of ^{7}Li and F atoms.

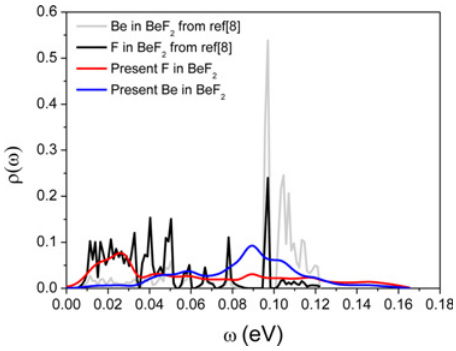

Figure 3. The calculated partial PDOSs of Be and F atoms.

crystal, the model used a $2 \times 2 \times 2$ supercell composed of 72 atoms. The k-point meshes in the full edge of the Brillouin were sampled by $8 \times 8 \times 8$. Figure 2 shows the calculated partial POSs of ^{7}Li and F atoms for ^{7}LiF, Fig. 3 shows the calculated partial POSs of Be and F atoms for BeF_2.There both were compared with the result from Mei and Cai [8].

Obviously, the calculated partial PDOSs of LiF are similar as the result from Mei and Cai [8], but the calculated partial PDOSs of BeF2 are different. BeF_2 crystal is low symmetrical crystal, need more supercell in the calculation to get the reasonable result. The same method were used to calculate the PDOSs, however different codes and initial inputs were used. To validate these, more experimental data are needed.

3.2. Thermal neutron scattering data

Based on the PDOS given above, and the bound atom scattering cross section given in Table 1 [25], the thermal neutron scattering law data were calculated using SIRIUS code. Here the incoherent approximation was used in inelastic scattering.

According to the bound atom cross section, the incoherent cross section and coherent cross section are same important for ^{7}Li, So the thermal neutron scattering data for ^{7}LiF crystals were divided into four parts. The

Table 1. Bound atom cross section.

	Coherent cross section	**Incoherent cross section**
^{7}Li	0.619b	0.78b
^{19}F	4.017b	0.0008b
^{9}Be	7.63b	0.0018b

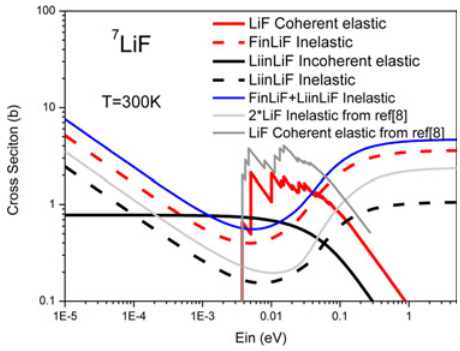

Figure 4. The thermal neutron scattering cross sections of ^{7}LiF at 300 K.

Table 2. Effective Temperatures and Debye- Waller integrals divided by the atomic mass for ^{7}LiF crystal.

T (K)	**^{7}Li in ^{7}LiF**		**F in ^{7}LiF**	
	W(eV^{-1})	**T_{eff} (K)**	**W(eV^{-1})**	**T_{eff} (K)**
300	6.573541	393.3	5.855736	343.4
400	8.273707	472.2	7.616744	433.1
500	10.04720	558.7	9.408490	526.7
600	11.86065	649.4	11.21623	622.4
700	13.69800	742.5	13.03331	719.2

first part was the coherent elastic scattering data for the whole ^{7}LiF crystal. The second part was the incoherent inelastic scattering data for F in ^{7}LiF. The third part was the incoherent inelastic scattering data for ^{7}Li in ^{7}LiF. The last part was the incoherent elastic scattering data for ^{7}Li in ^{7}LiF. In this work, the interference effects in inelastic didn't considered, and the same in BeF_2. Figure 4 shows the thermal neutron scattering cross section for ^{7}LiF crystal compared with the result from Mei and Cai [8] at 300 K.

Table 2 shows the result of effective temperatures and Debye-Wall integrals divided by the atomic mass for ^{7}LiF crystal.

For BeF_2 crystal, the incoherent cross section can be neglected, so the thermal neutron scattering law data for BeF_2 crystals were divided into three parts. The first part was the coherent elastic scattering data for the whole BeF_2 crystals. The second part and the third part were incoherent inelastic scattering data for Be in BeF_2 and F in BeF_2, respectively. Figure 5 shows the thermal neutron scattering cross section for BeF_2 crystal compared with the result from Mei and Cai [8] at 300 K.

Table 3 shows the result of effective temperatures and Debye-Wall integrals divided by the atomic mass for BeF2 crystal.

As showed in Fig. 4 and Fig. 5, the present scattering cross sections have significant difference with the Ref. [8]. For LiF crystal, the present PDOSs of Li and F are similar to the reference, but the present total inelastic scattering cross section is about twice as much as the reference. Maybe in the reference work, the input value of number

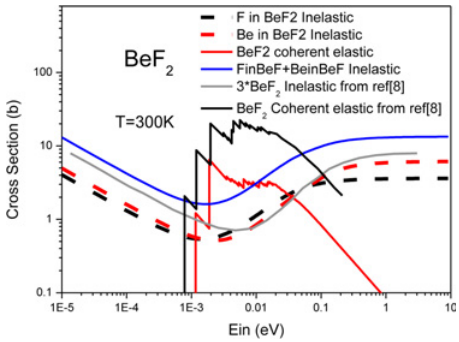

Figure 5. The thermal neutron scattering cross sections of BeF_2 at 300 K.

Table 3. Effective Temperatures and Debye- Waller integrals divided by the atomic mass for BeF_2 crystal.

T (K)	Be in BeF_2		F in BeF_2	
	$W(eV^{-1})$	T_{eff} (K)	$W(eV^{-1})$	T_{eff} (K)
300	6.819620	542.1	18.38910	472.4
400	8.762772	596.4	24.34908	541.1
500	10.74532	663.8	30.33266	618.5
600	12.75204	739.9	36.32943	701.6
700	14.77426	821.8	42.33428	788.8

of principal atoms in THERMR module for NJOY code was not set correctly. The difference in the elastic Bragg edges might be caused by the magnitude of reciprocal space vector. In NJOY code, the magnitude of reciprocal space vector for FCC structure is not the same as this work. For BeF2 crystal, difference of the fractional coordinates of atoms in unit cell and PDOSs are all the reasons, which cause the different scattering cross sections.

4. Conclusions

In summary, the thermal neutron scattering cross section for ^7LiF and BeF_2 crystals have been calculated in this work using a combination of ab-initio simulations, lattice dynamics, and SIRIUS code. Compared with the Ref. [8], obvious difference can be found in PDOSs and scattering cross sections, the possible cause which may lead these had been analysed in the previous section. However, to validate these calculated thermal neutron scattering data, experimental data are needed.

More work should be done in future. The first is to improve SIRIUS code for liquid materials. The second is to generate more thermal neutron scattering data for other materials such as silicon carbide and molten salt Flibe and so on.

This work was supported by Key Laboratory of Neutron Physics of CAEP (Grant No. 2013BA0, Grant No. 2013AA02)

References

[1] J.U. KOPPEL, J.R. TRIPLETT, Y.D. NALIBOFF, General Atomics report GA-7417 (1967)
[2] J.U. KOPPEL, D.H. HOUSTON, General Atomics report, GA-8774 (1978)
[3] R.E. MacFarlane, LA-12639-MS (1994)
[4] R.E. MacFarlane and D.W. Muir, LA-12740-M (1994)
[5] M.B. Chadwick, P. Oblozinsky, et al., Nuclear Data Sheets **107**, 2931 (2006)
[6] K. Shibata, O. Iwamoto, et al., J. Nucl. Sci. Technol. **48**, 1 (2011)
[7] A. Santamarina, D. Bernard, Y. Rugama, JEFF Report 22 (2009)
[8] L.W. Mei, X.Z. Cai, et al., J. Nucl. Sci. Technol. **50**, 419 (2013)
[9] L.W. Mei, X.Z. Cai, et al., J. Nucl. Sci. Technol. **50**, 682 (2013)
[10] J. Wang, H.Z. Song, et al., Nuclear Power Engineering **s2** (2014)
[11] G.L. Squires, Cambridge University Press (2012)
[12] D.E. Parks, M.S. Nelkin, J.R. Beyster, N.F. Wikner, W.A. BENJAMIN, INC (1970)
[13] MacFarlane, R.E., LA-12639-MS, 1994
[14] Shungo IIJIMA, J. Nucl. Sci. Technol. **3**(4), 160–164 (1966)
[15] G.M. Borgonovi, D. Sprevak, Nucl. Sci. and Eng. **42**, 137–142 (1970)
[16] I.I. Al-Qasir, A. I. Hawari, Trans. Am. Nucl. Soc. **96**, 660–661 (2007)
[17] A.I. Hawari, Nuclear Data Sheets **118**, 172–175 (2014)
[18] M.A. Zwijnenburg, F. Cora, R.G. Bell, J. Am. Chem. Soc. **130**, 11082 (2008)
[19] G. Dolling, R. Smith, et al., Phys. Rev. **168**, 970 (1968)
[20] P. Ghalsasi, P.S. Ghalsasi, Inorg. Chem. **50**, 86 (2011)
[21] A.D. Woods, W. Cochran, B.N. Brockhouse, Phys. Rev. **119**, 980 (1960)
[22] A.M. Karo and J.R. Hardy, Phys. Rev. **129**, 2024 (1963)
[23] G. Kresse, and J. Furthmuller, "Vienna Ab-Initio Simulation Package, VASP the Guide," (2002)
[24] K. Parlinski, "PHONON manual, version 3.11," (2002)
[25] Koester L, Neutron News **3**(3), 29–37 (1992)